Lateral Zoning of Groundwater Chemistry and Authigenic Mineralogy in the Oxfordian Regional Reservoir of the Nadym–Taz Interfluve

D.A. Novikov [a,b,] ✉, L.G. Vakulenko [a,b], P.A. Yan [a]

[a] *A.A. Trofimuk Institute of Petroleum Geology and Geophysics, Siberian Branch of the Russian Academy of Sciences,
pr. Akademika Koptyuga 3, Novosibirsk, 630090, Russia*

[b] *Novosibirsk State University, ul. Pirogova 2, Novosibirsk, 630090, Russia*

Abstract—This is a pioneering study on lateral zoning of groundwater chemistry and authigenic mineralogy in the Oxfordian regional reservoir of the Nadym–Taz interfluve. According to thermodynamic calculations, the nonequilibrium–equilibrium water–rock system lacks equilibrium with primary magmatic minerals, such as albite, anorthite, and microcline, though the water is moderately saline (up to 63.3 g/L) and has been in interaction with rocks for ~165 million years. Authigenic minerals form continuously and successively (kaolinite–montmorillonite–illite–micas–chlorite–albite–microcline) from waters that have certain pH and contents of SiO_2, Al, Na, K, Ca, and Mg. The equilibrium of groundwater with primary aluminosilicate minerals impinges on a carbonate barrier, and almost all rocks are more or less strongly carbonatized. Authigenic mineral assemblages from the southern Nadym–Taz interfluve include kaolinite unlike those from the northern part of the region, where albitization is more common. Authigenesis generally decays in the eastern direction.

Keywords: lateral zoning, authigenic minerals, groundwater chemistry, water–rock system, water–mineral complex, catagenesis, Upper Jurassic, West Siberia, Arctic

INTRODUCTION

Postdepositional alteration of subsiding sediments and its nature and mechanisms are among most important issues in basin studies. Alteration of sediments has been often studied by lithological methods while the physicochemical mechanisms remain poorly understood without due regard to groundwater chemistry.

Mikhail Lomonosov in his book *On the Strata of the Earth* written in the late 1750s (Lomonosov, 2012) considered rock formation processes as largely controlled by interaction with groundwater (a "natural solution"). Later, in the 1920s, Vladimir Vernadsky, who was at the origin of hydrogeochemistry, again stressed the key role of water in geological processes and specifically in mineral formation and alteration.

The water-rock system is intrinsically controversial being at the same time in and off the thermodynamic equilibrium: the principle substantiated thirty years ago in the Siberian science school of hydrogeochemistry leaded by S.L. Shvartsev. This controversy drives self-going prolonged continuous evolution of the water-rock system, with formation of new secondary minerals and related waters of new chemical types, which jointly make water-mineral complexes (Shvartsev, 1995, 2008).

The basic problem of water-rock interaction has been largely discussed for decades in the literature and at international conferences (Frape et al., 1984; Helgeson et al., 1993; Foustoukos et al., 2008; Scislewski and Zuddas, 2010; Hüpers et al., 2016; Wanner et al., 2017). Lithologists study alteration of water-, oil-, and gas-bearing rocks, formation of various cements, effects of postdepositional alteration on reservoir properties of rocks, etc. (Kossovskaya and Shutov, 1963; Rex, 1966; Perozio, 1971; Proshlyakov, 1974; Wilson and Pittman, 1977; McDowell and Elders, 1980; Kholodov, 1982a,b; Makhnach, 1989, 2000; McBride, 1989; Sakhibgareev, 1989; Lebedev, 1992; Stewart et al., 1994; Wilkinson et al., 2004; Yapaskurt, 2008; Zhao et al., 2011; etc.).

Zoning of Mesozoic sediments in the West Siberian basin according to authigenic mineralogy was a subject of several publications (Chernikov, 1969; Perozio, 1971; Ushatinsky and Zaripov, 1978; Predtechenskaya, 2010; etc.). Some concern vertical zoning in long drill sections from the Nadym–Taz interfluve, mainly those of the Tyumen superdeep borehole (TSG-6) with well documented core (Zonn and Dzyublo, 1990; Yapaskurt et al., 1992, 1997; Predtechenskaya et al., 1993, 2000; Kazansky et al., 1995; Yapaskurt and Gorbachev, 1996; Sirotenko and Gorbachev, 2000; Yapaskurt and Shikhanov, 2007; Sirotenko, 2009; etc.). Meanwhile, studies of lateral zoning are most often restricted to effects associated with oil and gas accumulations.

✉Corresponding author.
E-mail adress: NovikovDA@ipgg.sbras.ru (D.A. Novikov)

A wealth of data gained since the 1950s on compositions of pore fluids and on mineralogy and petrography of Mesozoic sediments in the West Siberian basin has extended and updated the existing ideas on some features of petroleum basins. Yet, the factors that control groundwater chemistry and authigenic mineralogy zoning remain unclear. We are trying to bridge the gap by this study, which is the first attempt of using an integrate approach to the problem for a specific reservoir.

MATERIALS AND METHODS

The Oxfordian regional reservoir, with its petroliferous permeable bed U_1, was chosen for this study as being the most exhaustively investigated by geological and geophysical methods among Jurassic basins. The study area is located within the Nadym–Taz interfluve in northern West Siberia (Fig. 1). In terms of hydrogeology, the Oxfordian reservoir corresponds to the Upper Jurassic aquifer which

belongs to the lower hydrogeological stage according to the conventional division (Kruglikov et al., 1985; Shvartsev and Novikov, 2004; Matusevich et al., 2005; Novikov and Lepokurov, 2005; Novikov, 2017a). We studied mineralogy and petrography in shelf or (less often) coastal sands from the Upper Vasyugan and Lower Sigovaya subformations at core depths 2720–3870 m. The sands have slightly altered polymictic compositions of the detrital component with fine to medium grain sizes (Yan and Vakulenko, 1998; Yan, 2001). On the regional scale, the Vasyugan Formation sediments have reached the latest middle-earliest late stage of maturity (Predtechenskaya et al., 2015), with the thermal maturity of kerogen (catagenesis) corresponding to grades MC_1^2 in the south, MC_2 in the north, and MC_1^1 in the east (Fomin, 2011). We used data from reference sections of the Tyumen superdeep (SG-6) and West Novogodnyaya 210 boreholes in the northern and southern Nadym–Taz interfluve, respectively.
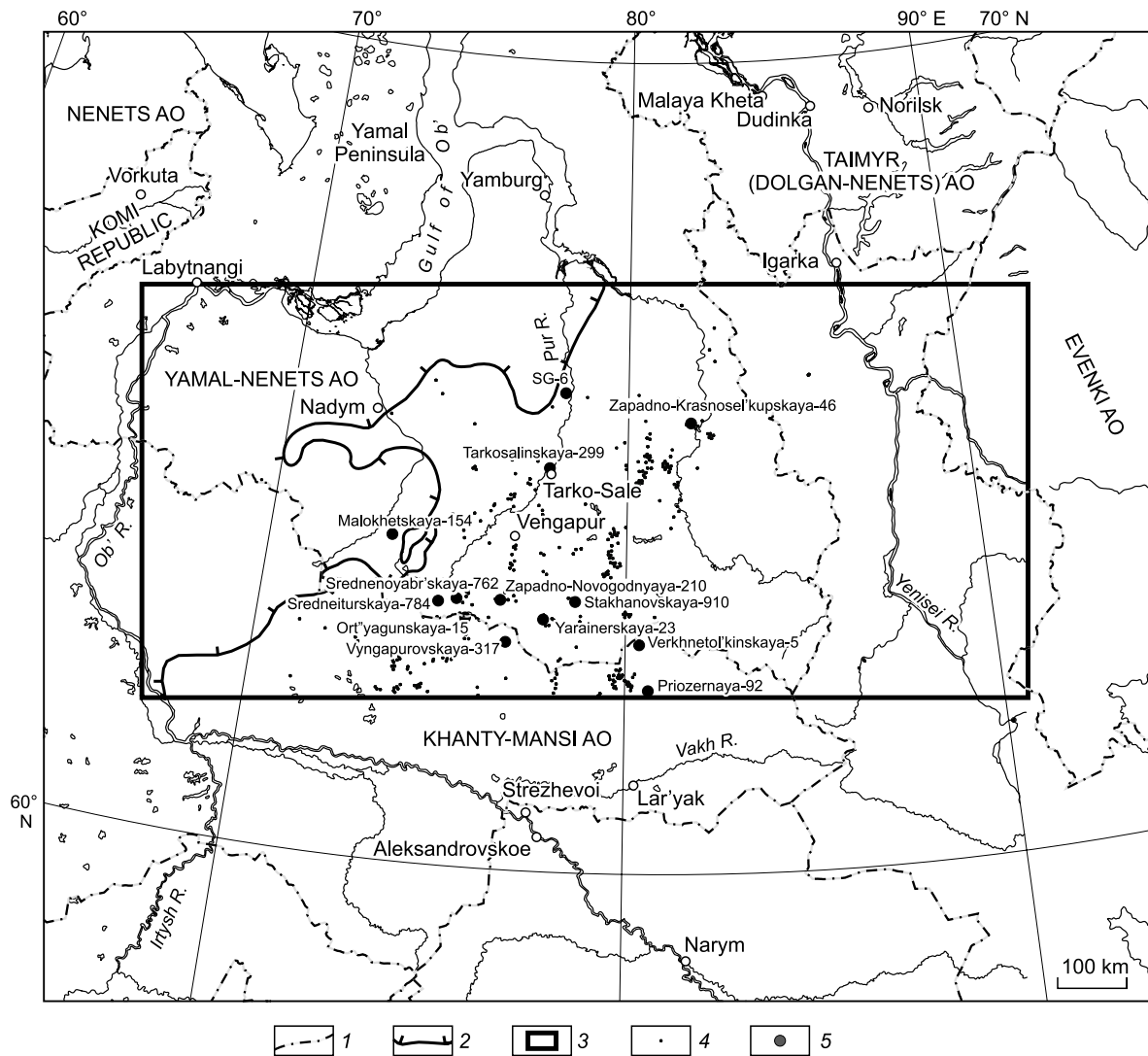

Fig. 1. Location map of study area in northern West Siberia. *1–3*, boundaries: administrative (*1*), clay alteration of Oxfordian regional reservoir (*2*), study area (*3*); *4, 5*, boreholes sampled for groundwater chemistry (*4*) and authigenic minerals (*5*).

Table 1. Main parameters of groundwater chemistry in Upper Jurassic aquifers

Major ion, mg/L	Values					Median	Standard deviation	Standard error	Number of analyses
	min	Background	max	Confidence interval					
				min	max				
M*	2.0	19.9	63.3	19.0	20.9	16.9	11.9	0.5	644
pH	6.2	7.6	8.3	7.4	7.6	7.5	1	0.1	423
Na^+	891	6336	24,521	5999	6674	5429	3886	172	644
K^+	3	115	502	107	123	100	79	4	351
Ca^{2+}	8	502	3250	463	542	316	500	20	622
Mg^{2+}	1	62	547	57	67	39	61	3	581
SO_4^{2-}	1	33	248	28	37	21	35	2	232
Cl^-	780	11,271	37,600	10,695	11,847	9574	7351	293	644
HCO_3^-	12	834	3709	786	882	708	611	25	644
I^-	0.4	5.2	45.0	4.6	5.8	3.4	6.6	0.3	498
Br^-	6.7	40.5	207.9	38.1	43.0	36.7	27.7	1.2	511
B^+	0.3	9.0	200.0	8.2	9.7	7.2	8.2	0.4	472
NH_4^+	0.2	39.4	150.0	33.0	45.9	30.0	33.0	3.3	102
Naphthanoic acids	0.1	0.6	4.0	0.4	0.7	0.4	0.6	0.1	87
SiO_2	3.0	25.8	86.0	21.6	29.9	21.0	18.0	2.1	75
F^-	0.3	1.2	8.9	1.1	1.4	1.1	0.7	0.1	86
Sr^{2+}	24.6	94.6	1320.0	3.7	45.1	16.6	24.8	8.8	38

* Total salinity (TDS), g/L.

The groundwater chemistry data we used were collected for a long period of time and required careful selection and statistical processing to pick background and anomalous parameter values (Table 1) and to calculate the conventional coefficients. The data were processed in Microsoft Excel, STATISTICA, SURFER, GridBuilder-GridMaster, and Rockworks. The electronic database for the Oxfordian reservoir in the Nadym–Taz interfluve includes testing and sampling results from 537 objects (644 samples). Further work focused on main hydrogeochemical features of groundwaters in Upper Jurassic sediments as a basis for respective maps, as well as on equilibrium in the water-rock system. The equilibrium was estimated by thermodynamic calculations using the HydroGeo software which can account for water salinity up to brine concentrations (Bukaty, 1999).

Pore waters interact with carbonate minerals (calcite and dolomite) by the congruent dissolution reaction: $MCO_3 + H^+ = M^{2+} + HCO_3^-$. Incongruent dissolution of aluminosilicate minerals, mainly associated with hydrolysis, occurs as (Drever, 1988)

$$MSiAlO_n + H_2O = M^{n+} + OH^- +$$

$$[Si(OH)_{0-4}]_n + [Al^o(OH)_6]_n^{3-}$$

or $Al(OH_3) + (M, H) Al^o SiAl^t O_n,$
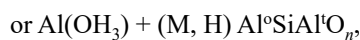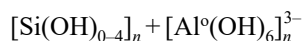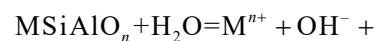
where n are the indefinite atomic ratios; o and t are the octahedral and tetrahedral sites, respectively; M stands for any metal cation; and the last term of the reaction (M, H) $Al^o SiAl^t O_n$ stands for clay minerals, zeolite, and aluminosiliciclastic material.

Reference data on groundwater chemistry were borrowed from (Helgeson, 1969; Ben Baccar and Fritz, 1993) for the systems $HCl–H_2O–Al_2O_3–CO_2–MgO–Na_2O–SiO_2$ and $HCl–H_2O–Al_2O_3–CO_2–MgO–K_2O–SiO_2$, and from (Silkina, 2001; Silkina and Zhukovskaya, 2002) for $SiO_2–Al_2O_3–Na_2O–CO_2–H_2O$, $SiO_2–Al_2O_3–CaO–CO_2–H_2O$ and $SiO_2–Al_2O_3–K_2O–CO_2–H_2O$. The equilibrium lines in phase diagrams for Na, Ca, and K aluminosilicates plotted by the method of Garrels and Christ (1965) are similar to those in the diagrams reported by Ben Baccar and Fritz (1993) and Garrels and Christ (1965) for 100 ºC and by Helgeson (1969) and Aagaard and Helgeson (1982) for 25 °C and 100 °C. The position of the lines in the diagrams is very sensitive to errors in Gibbs free energy values for minerals (Drever, 1988).

RESULTS AND DISCUSSION

Hydrogeological background. The Upper Jurassic aquifer (Oxfordian regional reservoir) consists of shelf and coastal sand and silt and varies in total thickness from 80 to 260 m increasing eastward from 80–110 m in the Northern arch to 240–260 m in the Krasnyi Sel'kup monocline (Fig. 2).

Previous studies revealed the principle fluid dynamic pattern of the area with latent groundwater discharge in the West Siberian basin (Kruglikov et al., 1985; Matusevich et al., 2005) and two main regional-scale flows: water expulsed upon sediment compaction in the west, from the clay alteration boundary, and percolated water in the east, from
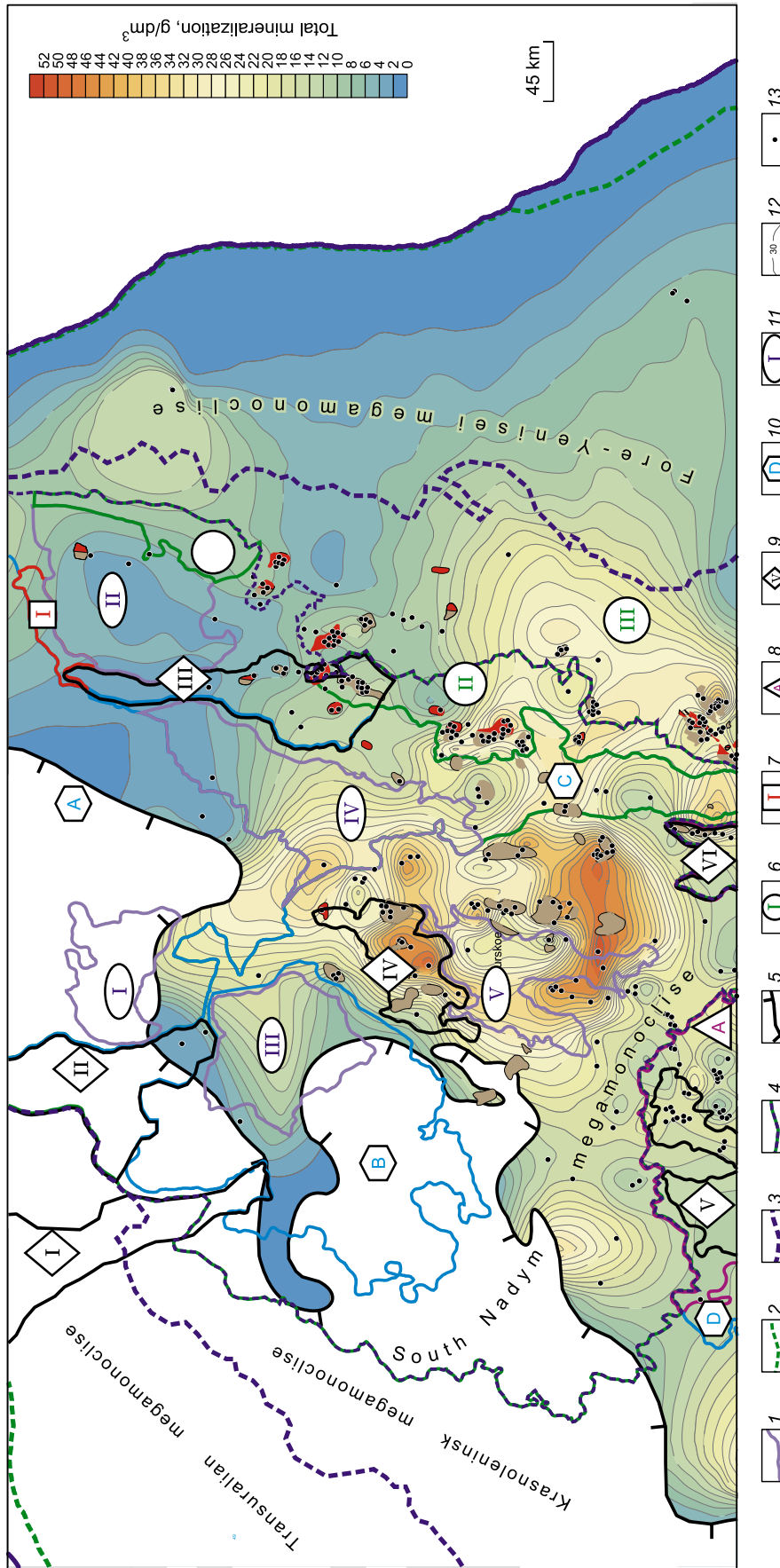
Fig. 2. Total salinity (TDS) of groundwaters in the Oxfordian regional reservoir, Nadym–Taz interfluve. *1–5*, boundaries of West Siberian basin (*1*), Jurassic sedimentary basin (*2*), Inner area and Outer belt (*3*), Yamal–Kara basin (*4*), clay alteration of Oxfordian regional reservoir (*5*); *6*, monoclines of large and medium scales (first and second order structures); East Taz monocline (I), East Pur monocline (II), Krasnyi Sel'kup monocline (III); *7*, first-order North Chasel'ka saddle (I); *8, 9*, positive tectonic elements: zero-order Khantei hemianticlinal uplift, A (*8*), first-order structures (*9*): North Gydan uplift (I), Yarudei uplift (I), Medvezh'e–Nuga inclined swell (II), Chasel'ka inclined swell (III), Northern arch (IV), Surgut arch (V), Variegan–Tagra uplift (VI); *10, 11*, negative tectonic elements: zero-order structures (*10*): A, Bol'shaya Kheta basin; B, Nadym hemisynclinal basin; S, Middle Pur inclined trough; D, Mansi synclinal basin; first-order structures (*11*): I, Neruta basin; II, Taz structural embayment; III, Upper Tanlov basin; IV, Middle Pur inclined trough; V, Pyakupur–Amputa inclined trough; *12*, contour lines; *13*, boreholes.

the basin periphery. The pattern is the same in the Upper Jurassic aquifer, where pore pressure varies from 9.9 to 67.7 MPa and is anomalously high, with an overpressure ratio of $K_a = 1.87$ (Novikov, 2018; Novikov et al., 2018a). Fluid dynamic stress analysis in the Nadym–Taz interfluve reveals two zones: normal pressure in the east, overpressure in the western and central parts, and an N–S zone of moderately high pressure ($K_a = 1.05$–1.15) between them. Sporadic fluid dynamic anomalies with high pressure (moslty hydrostatic component), occur in the eastern part of the area within the Yutyrmal, Tekto-Kharampur, and Ravninnoe oil and gas fields (Shvartsev and Novikov, 2004; Novikov, 2017b). The existence of a large overpressure zone in the central and western Nadym–Taz interfluve, near the clay alteration boundary in the Oxfordial reservoir, is due to the regime of water explusion from compacted sediments (Shvartsev and Novikov, 2004; Novikov and Lepokurov, 2005; Novikov, 2018; Novikov et al., 2018a).

Maximum pressures normalized to the 3800 m depth within the Upper Jurassic aquifer are reasonably associated with structures in the Middle Pur inclined trough and the Bol'shaya Kheta basin. The total pressure gradient across the aquifer reaches 34.0 MPa. Judging by higher normalized pressures at the clay alteration boundary in permeable deposits, lateral W–E migration of fluids may be driven by lithostatic fluid pressure associated with explused water under a tight lithological screen. Main pressure minimums likewise fit the contours of large oil and gas fields (e.g., Kharampur) within the Middle Pur inclined trough and other structures.

The two types of water flow meet in the zone of the Koltogory–Urengoi paleorift and discharge by vertical cross flow along faults. This process is recorded in the fluid pressure pattern and becomes evident within the Northern arch and some other structures where zones of overpressure while moderately high pressures exist as far as the lowest Aptian–Albian–Cenomanian aquifers (Shvartsev and Novikov, 2004; Novikov and Lepokurov, 2005; Novikov, 2017a,b, 2018). Groundwaters in pre-Mesozoic, Triassic, and Jurassic rocks discharge into the overlying sediments by successive vertical cross flow. They show an intricate vertical zoning according to water salinity, with a large zone of brackish waters (10–15 g/L): salinity decreases with depth in the northern part of the Nadym–Taz interfluve but shows a complex depth dependence in the south, where the downward decrease is minor within the 1000–2500 m depths but prominent between 2800–3200 m and becomes reverse below 3200 (Lower Jurassic sediments), though not in all structures (Shvartsev and Novikov, 2004; Novikov et al., 2017a).

Major-ion chemistry and its lateral zoning. Groundwaters in the study area vary in major-ion chemistry, with predominant chlorine-sodium (Cl–Na), chlorine-bicarbonate-sodium (Cl–HCO$_3$–Na) and bicarbonate-chlorine-sodium (HCO$_3$–Cl–Na) compositions, according to the classification of Schukarev (Samarina, 1977) and a total salinity of 5 to 63.3 g/L TDS (Shvartsev and Novikov, 2004; Novikov

and Lepokurov, 2005; Novikov, 2017a; Novikov et al., 2018b). Each water type has its specific distribution of major and minor salt-forming components correlated with TDS. Representative analyses of main chemical water types (Table 2) show regular increase in major ions of Cl$^-$, Na$^+$, Mg^{2+}, Ca^{2+}, K$^+$, as well as in minor components of Br$^-$, I$^-$, NH$_4^+$, and Sr^{2+} from bicarbonate-chlorine-sodium to chlorine-sodium compositions. More saline waters (15–20 g/L TDS or more) contain less 2HCO$_3^-$. The contents of SO$_4^{2-}$, which reduces to H$_2$S (SO$_4^{2-} + 2C_{org} + 2H_2O = 2HCO_3^- + H_2S$), average about 20 to 60 mg/L.

There are three prominent salinity peaks within the region: one (31–36 g/L) in the Kholmistaya area (southern Krasnyi Sel'kup monocline) and two more (39–64 and 41–59 g/L) in the Izvestinskaya (Northern arch) and Aiva–Sedopur (South Nadym monocline) areas, respectively (Fig. 2). In general, water salinity decreases in the northern and northwestern directions, toward the clay alteration boundary, and to the northeast, toward the basin margin, where it is as low as 5–10 g/L. The same pattern appears as waters change from Cl–Na to Cl–HCO$_3$–Na compositions, with predominant ions of Na$^+$ (20–24 g/L) and Cl$^-$ (30–37 g/L) in the former and 2HCO$_3^-$ in the latter (25–47 wt.% equivalent or 2–3 g/L TDS).

The regional-scale background salinity of waters in Upper Jurassic sediments is 19.9 g/L (Table 1). Salinity highs of >25 g/L occur within the Northern and Nizhnevartovsk arches and the East Pur and South Nadym monoclines, and also mark positive tectonic structures in the Inner Zone; the highest background values were observed in the Northern arch (33.5 g/L).

As the salinity increases, the characteristic element ratios in groundwaters (indicators of their alteration degree) become at least twice lower: from rNa/rCl = 2.20–3.09 at a salinity of 5–9 g/L to the respective range 0.85–0.88 at >25 g/L; Cl/Br and B/Br are, respectively, 400 and 3.09 at 5.1 g/L but 211–275 and 0.07–0.17at 25 g/L (Table 2, Fig. 3). However, the behavior of the rNa/(rCa + rMg) and Br/I ratios differs slightly from the general trend: rNa/(rCa + rMg) is the highest (50) at 5–10 g/L, then decreases to 5 in the most saline water; Br/I is 8.9 at a salinity of 15–20 g/L and decreases in more saline water; HCO$_3$/Cl shows the largest range, from 0.04 to 1.59.

More saline waters are less chemically diverse: seven types of waters with 2–5 g/L TDS, five types at 10–15 g/L, two types at 20–25 g/L, and only one sodium chloride type at >25 g/L (chemical types are according to Schukarev's classification (Samarina, 1977)).

According to Cl-normalized distribution of major cations (Na$^+$, Mg^{2+}, Ca^{2+}, and K$^+$), chemical types of water change from the most saline Cl–Na to HCO$_3$–Cl–Na types. The alteration degree of groundwaters and their affinity to seawater decrease in the same direction (Fig. 3).

Equilibrium in the water–rock system. Once water gets into a sedimentary basin, its chemistry begins to change upon interaction with rocks and disseminated organic mat-

Table 2. Groundwater chemistry in the Oxfordian regional reservoir, Taz interfluve: Representative analyses

Area/borehole/perfo-ration interval	pH	Major ion, mg/L														M g/L	$\frac{r\text{Na}}{r\text{Cl}}$	Cl/Br	B/Br
		Ca^{2+}	Mg^{2+}	Na^+	K^+	Cl^-	HCO_3^-	SO_4^{2-}	NH_4^+	B^+	Br^-	I^-	F^-	SiO_2	Sr^{2+}				
1	2	3	4	5	6	7	8	9	10	11	12	13	14	15	16	17	18	19	20
HCO_3–Cl–Na waters																			
Zapadno-Krasno-sel'kupskaya, BH 48, 3030–3070	6.5	40	18	1518	22.5	1064	2440	0	0.4	8.2	2.7	0.9	2.0	22.0	–	5.1	2.20	400	3.09
Kynskaya, BH 214, 2904–2908	8.9	22	7	2768	42.0	1383	4880	5	–	5.4	4.8	0.8	2.0	36.0	–	9.2	3.09	289	1.13
Mean value	7.7	24	13	2290	43	1948	3457	5	0.4	6.8	3.7	0.8	2.0	29	–	7.2	2.59	345	2.11
Cl–HCO_3–Na waters																			
Sidorovskaya, BH 35, 3390–3418	8.5	8	11	1125	16	1064	939	83	0.0	3.5	4.9	2.6	1.1	4.0	5.7	3.4	1.63	219	0.72
Yuzhno-Sidorovska-ya, 4, 3326–3348	8.7	12	8	1522	26	1241	1659	16	0.2	10.1	8.4	1.75	3.4	21	–	4.7	1.89	147	1.21
Novochasel'skaya, BH 222, 2952–2966	8.5	24	10	1564	19	1702	1378	17	0.7	23.6	3.8	1.7	2.4	15.0	2.4	4.8	1.42	449	6.23
Zapadno-Krasno-sel'kupskaya, 50, 2875–2880	8.0	46	5	1732	35	1453	2220	59	2.5	–	5.3	0.8	6.0	31.0	–	5.6	1.84	274	–
Verkhnechasel'skaya, 156, 2880–2942	7.9	62	12	2079	27	2411	1623	48	7.5	8.5	6.9	0.8	6.0	11.0	–	6.3	1.32	348	1.23
Kynskaya, BH 200, 2907–2910	8.1	48	11	2833	34	3103	2159	0	22.5	37.0	9.7	3.5	1.2	22.0	12.8	8.2	1.41	319	3.81
Mean value	8.2	36	9	2377	46	2377	2188	51	9.9	14.2	8.1	2.1	3.3	16.6	6.7	7.1	1.60	295	2.05
Cl–Na waters																			
Vostochno-Iokh-turskaya, BH 513, 3026–3030	7.4	650	61	11102	210	18,262	891	10	–	34.3	65.6	5.5	0.8	23.0	290.0	31.2	0.94	281	0.52
Kholmistaya, BH 667, 2926–2930	7.3	920	128	11142	170	18,794	695	6	90.0	18.6	64.8	6.6	0.9	56.0	370.0	31.8	0.91	290	0.29
Vostochno-Iokh-turskaya, BH 524, 2981–2988	7.2	564	129	12000	183	19,680	768	7	45.0	12.4	80.0	1.7	1.1	12.0	340.0	33.4	0.94	246	0.16
Kharampurskaya, BH 295, 2956–2958	6.4	1380	201	12333	200	21,631	671	8	30.0	7.8	82.3	2.6	–	20.0	435.0	36.4	0.88	263	0.09
Iokhturskaya, BH 525, 2982–2986	7.6	1638	134	12190	173	21,985	620	12	25.0	39.3	73.6	6.5	2.3	16.0	488.4	37.6	0.85	299	0.53
Izvestinskaya, BH 707, 2962–3010	7.3	1150	207	13714	200	23,049	781	7	75.0	14.3	83.7	13.1	0.5	39.6	450.0	39.1	0.92	275	0.17
Mean value	7.5	744	92	8953	139	14,906	754	26	37.9	13.4	46.5	3.7	1.4	25.6	219.8	25.6	0.95	295	0.44

Note. Dash, means no data.

ter. According to available data on groundwater equilibrium with carbonate minerals (calcite and dolomite), only few water points lie below saturation and represent conditions for dissolved elements at 25 °C, but all hotter waters are oversaturated with respect to calcite and dolomite which can precipitate as secondary phases from 80 to 100 °C waters. Since calcite is less soluble at higher temperatures, saturation is the highest in most deeply subsided basin parts. Dolomite shows the same behavior, though its solubility is orders of magnitude lower than in calcite.

The lack of equilibrium between groundwaters and primary aluminosilicate minerals is a key factor for the formation of secondary carbonates. The water-rock system being multi-component, saturation with respect to individual elements should be treated holistically. Incongruent dissolution, with all its complexity, is due mainly to hydrolysis (Shvartsev, 1991, 1998).

As shown by thermodynamic calculations (Fig. 4), groundwaters are almost off equilibrium with primary magmatic phases (albite, anorthite, and microcline) but are equilibrated with micas, illite, Ca-, Na- and Mg-montmorillonite, kaolinite, and less often Mg-chlorite (Novikov, 2012, 2016, 2017c).

The points for the system SiO_2–Al_2O_3–Na_2O–CO_2–H_2O are scattered (Fig. 4a) and fall within the stability fields of paragonite, Na-montmorillonite, and albite; formation of so-
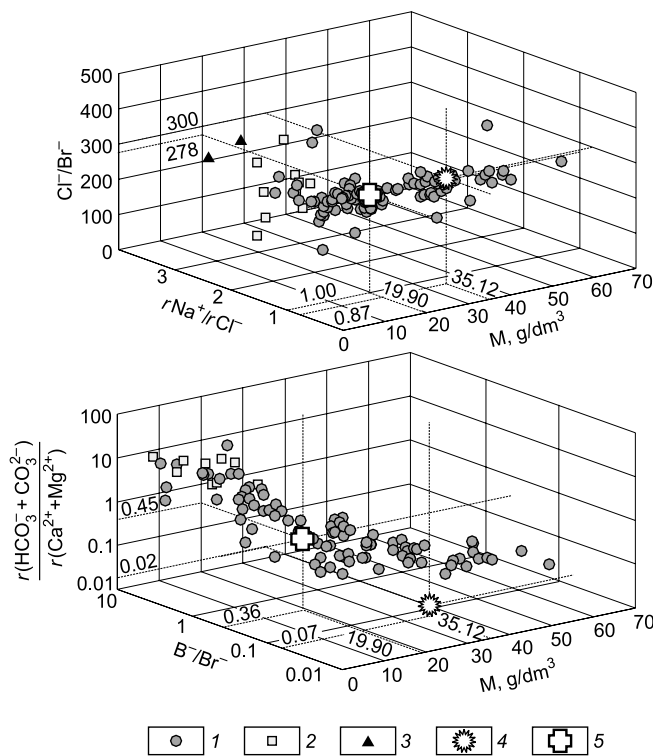
Fig. 3. Block diagrams of TDS-dependent ratios of components as indicators of groundwater alteration degrees. *1–3*, Chemical types of groundwater (after S. Schukarev (Samarina, 1977)): Cl–Na (*1*), Cl–HCO$_3$–Na (*2*), HCO$_3$–Cl–Na (*3*); *4*, *5*, ratios for seawater (*4*) and background water (*5*) compositions.

dic aluminosilicates (kaolinite, montmorillonite, and micas) is the most probable. In the case of another system SiO$_2$–Al$_2$O$_3$–CaO–CO$_2$–H$_2$O (Fig. 4*b*), almost all waters are within the stability fields of clay minerals and reach equilibrium with Ca-montmorillonite, kaolinite, and margarite (to a lesser degree). Dissolution of primary aluminosilicate minerals (anorthite) is attendant with the formation of clay minerals and micas. As for the system SiO$_2$–Al$_2$O$_3$–K$_2$O–CO$_2$–H$_2$O (Fig. 4*c*), most of points fit the stability of illite and muscovite and fewer points lie within the microcline stability. Hydrolysis of silicates is largely controlled by the content of silica compounds in groundwaters: illite forms at lower H$_4$SiO$_4$ while micas precipitate from more silicic waters.

Points corresponding to water equilibrium with magnesian minerals (Fig. 4*d*, *e*) plot densely and almost linearly toward the formation of Mg-montmorillonite and Mg-chlorite; some points fall within the stability fields of illite and albite. In the system HCl–H$_2$O–Al$_2$O$_3$–CO$_2$–MgO–Na$_2$O–SiO$_2$, most points fit the stability of Mg-chlorite and Mg-montmorillonite and few are within that of low-temperature albite, Na-montmorillonite, and kaolinite (Fig. 4*d*). This behavior is consistent with possible formation of secondary albite as the evolution of the water-rock system progresses. The most deeply subsided parts of the northeastern Nadym–Taz interfluve (Kyn, Novaya Chasel'ka and other areas) approach this stage of evolution. The general tendency is in-

creasing saturation of waters with respect to relatively low-temperature albite upon growth of pH and dissolved silica contents. Like the previous cases, most points for the system HCl–H$_2$O–Al$_2$O$_3$–CO$_2$–MgO–K$_2$O–SiO$_2$ fall within the stability fields of Mg-chlorite, Mg-montmorillonite, and illite (Fig. 4*e*).

In general, thermodynamic calculations show that groundwaters in the Upper Jurassic aquifers are saturated with carbonate minerals. On the other hand, water is unsaturated with respect to primary aluminosilicate minerals which experience continuous dissolution (Fig. 4). As a result, the Ca^{2+}, Mg^{2+}, Na$^+$, K$^+$, Al$_2$O$_3$, and H$_4$SiO$_4$ are bound in secondary (authigenic) minerals. The latter are stable at this stage of the system evolution, and their equilibrium with groundwaters limits the increase of dissolved cations. On the other hand, water in the Upper Jurassic sediments contains decayed organic matter, while the dissolved CO$_2$ and organic acids neutralize alkalis released by hydrolysis of aluminosilicates; thus, the latter are not equilibrated with the water. The newly formed products of the system are stable against the aggressive action of groundwaters.

The system evolution is mainly controlled by pH and amount of dissolved silica. The pH values and H$_4$SiO$_4$ increase progressively in groundwater equilibrated with phases that form a series from clay minerals to magmatic aluminosilicate phases in the course of the system evolution in the zone of supergene alteration (Shvartsev et al., 2007). The Nadym–Taz groundwaters of the Oxfordian regional reservoir that are in equilibrium with different secondary (or occasionally primary) aluminosilicate minerals differ in their major-ion chemistry (Table 3). In our previous studies (Novikov, 2012, 2016, 2017c), we found out that widespread kaolinite cement forms at pH = 7.2 on average and at 15–20 mg/L silica, while authigenic albite precipitates at 40–80 mg/L silica and pH about 8.2–9.0. Different contents of cations (K$^+$, Na$^+$, and Mg^{2+}) in groundwaters equilibrated with aluminosilicate minerals result from quantitative and qualitative variations in their binding with clay minerals and micas (Novikov, 2016, 2017c). Thus, the composition difference of groundwaters equilibrated with certain aluminosilicates and carbonates means that new minerals precipitate from waters of certain compositions in respective environments.

Saturation of groundwaters in aluminosilicate minerals has implications for main trends in the water-rock evolution (Fig. 5). Interaction of waters with their host sediments in the northern Nadym–Taz interfluve is at a later evolutionary stage than in the south of the region, judging by shifts in phase diagrams. Waters in Upper Jurassic sediments are in equilibrium with clay minerals: kaolinite and montmorillonite in the systems SiO$_2$–Al$_2$O$_3$–Na$_2$O–CO$_2$–H$_2$O and SiO$_2$–Al$_2$O$_3$–CaO–CO$_2$–H$_2$O, and with illite in the system SiO$_2$–Al$_2$O$_3$–K$_2$O–CO$_2$–H$_2$O. In the systems SiO$_2$–Al$_2$O$_3$–Na$_2$O–CO$_2$–H$_2$O and SiO$_2$–Al$_2$O$_3$–K$_2$O–CO$_2$–H$_2$O of waters from more deeply subsided sediments, the shifts are prominent in the field of feldspars (albite and microcline). Earlier we re-

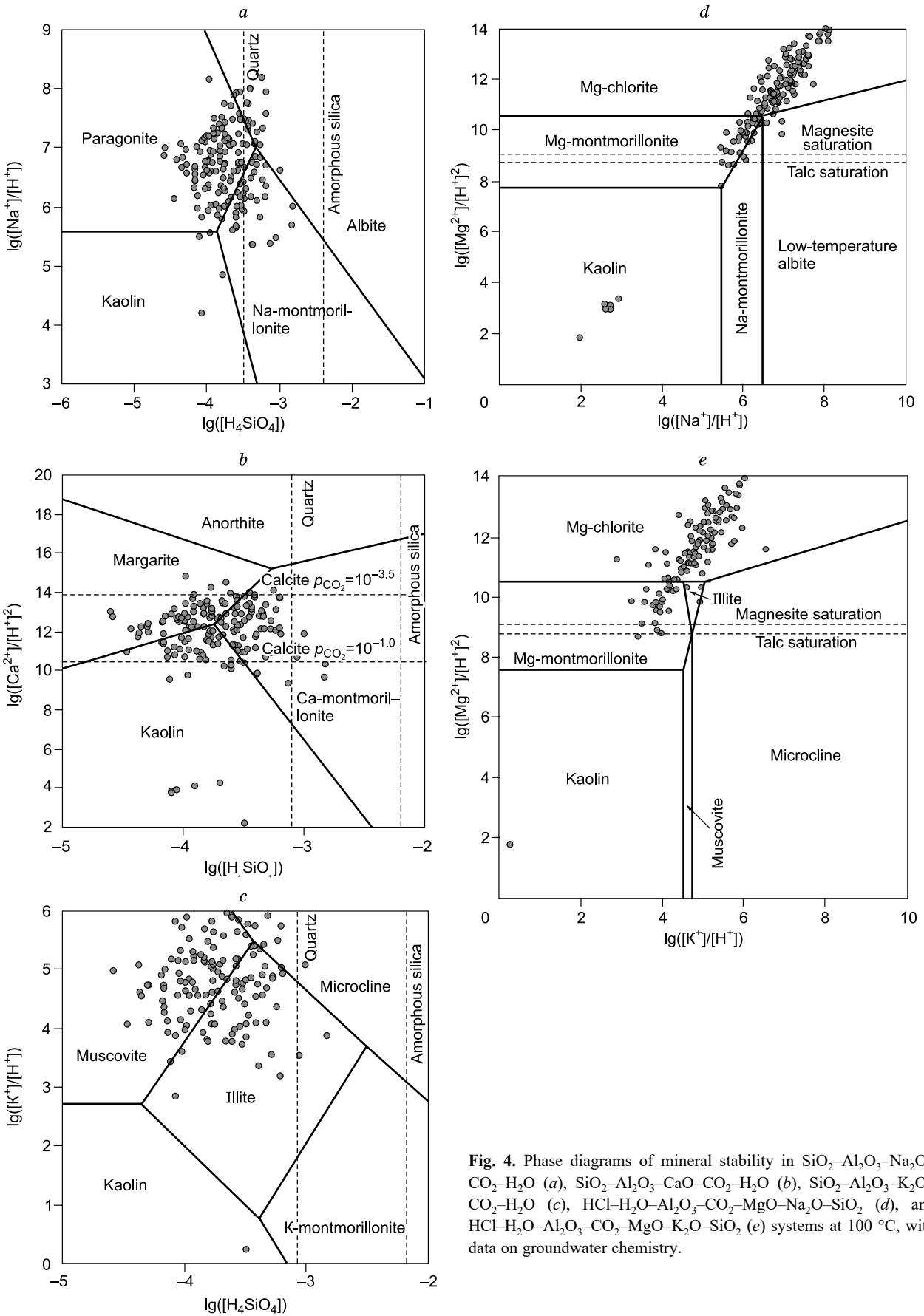**Fig. 4.** Phase diagrams of mineral stability in SiO_2–Al_2O_3–Na_2O–CO_2–H_2O (*a*), SiO_2–Al_2O_3–CaO–CO_2–H_2O (*b*), SiO_2–Al_2O_3–K_2O–CO_2–H_2O (*c*), HCl–H_2O–Al_2O_3–CO_2–MgO–Na_2O–SiO_2 (*d*), and HCl–H_2O–Al_2O_3–CO_2–MgO–K_2O–SiO_2 (*e*) systems at 100 °C, with data on groundwater chemistry.

Table 3. Average major-ion chemistry of groundwaters equilibrated with aluminosilicate minerals, Oxfordian reservoir, Nadym-Taz interfluve

Mineral	Equilibrium major ion contents, mg/L						
	pH	Ca^{2+}	Mg^{2+}	Na^+	K^+	HCO_3^-	H_4SiO_4
Kaolinite	7.2	630	142	8009	118	901	20.6
Mg-montmorillonite	6.8	588	54	7014	96	860	28.2
Sa-montmorillonite	7.7	290	28	5317	85	1159	32.2
Na-montmorillonite	6.9	552	41	7170	120	836	37.5
Illite	7.5	458	48	6348	93	961	30.4
Margarite	8.1	351	84	5354	99	940	20.4
Paragonite	7.8	394	99	5782	97	989	22.6
Muskovite	7.8	340	125	5362	101	971	24.0
Mg-chlorite	8.2	414	115	5068	89	1174	44.3
Albite	8.6	112	18	4373	63	1504	62.4
Microcline	8.7	30	13	3294	50	1720	86.3

ported a similar trend for the Nyurol'ka basin and deep strata of the northern West Siberian basin, like the Kharampur swell, etc. (Zhukovskaya and Novikov, 2002; Novikov, 2016, 2017c).
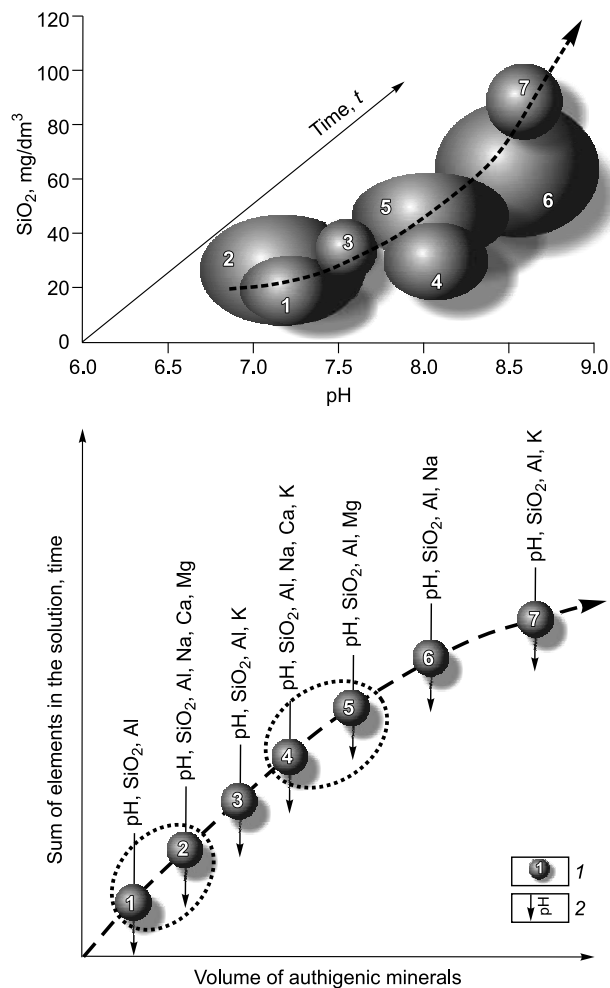

Fig. 5. Successive changes in water-mineral complexes in zone of catagenesis, northern West Siberian basin. *1*, water-mineral complexes: kaolinite (1), montmorillonite (2), illite (3), mica (4), chlorite (5), albite (6), microcline (7); *2*, chemical parameters of material that control authigenic mineral formation.

Lateral authigenic-mineralogical zoning. The question arises whether authigenic minerals from the host sediments in the Oxfordian reservoir exhibit any influence of groundwater chemistry and whether their compositions vary laterally over the region. Data on mineralogy and petrography show that silts and sands from different areas bear almost the same authigenic minerals, but of different relative percentages and alteration degrees. The minerals are abundant carbonates (calcite, siderite, dolomite), less abundant quartz, chlorite, kaolinite, illite, and pyrite, and minor albite and Ti-bearing minerals (anatase, leucoxene).

We additionally estimated some quantitative parameters which characterize postdepositional alteration of core samples from least carbonatized sandstone sections: number of regenerated detrital quartz particles and relative percentages of strongly, moderately, and weakly altered (or fresh) detrital feldspar particles.

A 17 m thick silt-sand bed in the upper part of the Upper Vasyugan subformation (core depth 3855–3872 m, Tyumen superdeep borehole) contains no more than 10–15% carbonate-clay cement in its upper half and several levels of high contents of secondary calcite; fine or very fine calcite reaches 30–40% and causes corrosion in most of clasts and replaces some of them. Later dolomite exists as few fine rhombohedral crystals. Detrital quartz particles are mostly not regenerated (46 to 63%), but regenerated particles, with regeneration rims, are occasionally quite abundant in coarser rocks (Fig. 6*A*, *B*, *C*). Feldspars (mainly high-silica plagioclase) are altered to different degrees: pelitized or less often sericitized. Albite forms thin regeneration rims (Fig. 6*A*) but is rarely authigenic (within 0.5%). The relative percentages of alteration degrees in feldspars are: 49–64% weak (or zero), 39–45% moderate, and 5–6% strong. Some plagioclases underwent cataclasis and few grains show plastic deformation of polysynthetic twins. Authigenic pyrite (fractions of percent to 5%) and Ti phases (fractions of percent anatase and leucoxene) are ubiquitous along the section.

We studied the Upper Vasyugan subformation in several areas of the southern Nadym–Taz interfluve. In the Zapad-
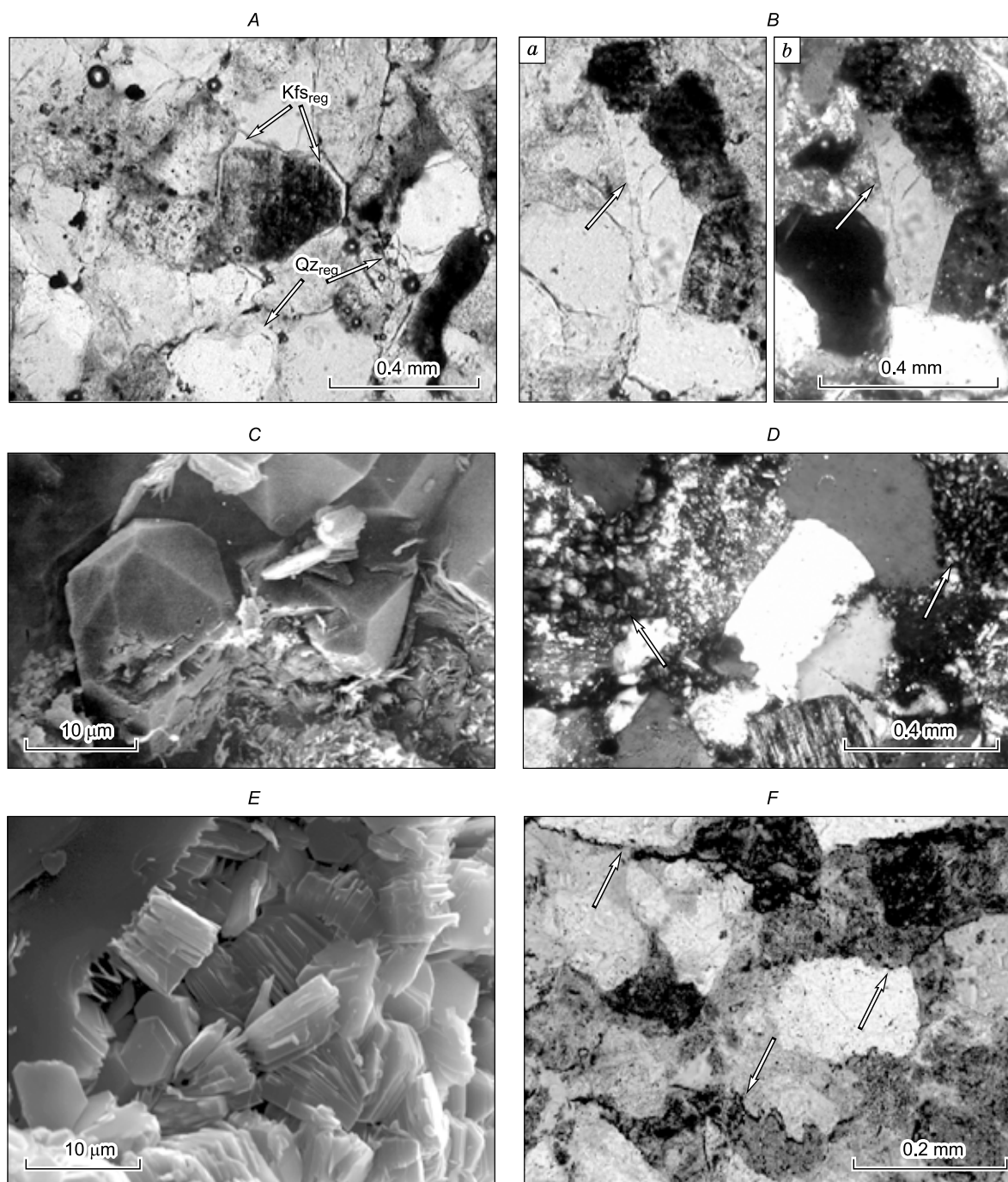
Fig. 6. Plate 1. *A*: regeneration of strongly altered feldspar and quartz, borehole SG-6, depth 3863.3 m. Plane polarized light image. *B*, regeneration rim in a quartz clast, borehole SG-6, depth 3871.2 m. Plane (*a*) and cross (*b*) polarized light images; *C*, quartz clasts regenerated to euhedral crystals, borehole SG-6, depth 3871.2 m; *D*, very fine, fine, and coarse flaky more or less strongly recrystallized interstitial kaolinite, borehole ZN-210, depth 3196 m. Cross polarized light image; *E*, interstitial kaolinite that replaces rims of K-feldspar clasts, borehole ZK-46, depth 2790 m; *F*, visible stylolite sutures at grain boundaries in detrital sandstone, borehole ZK-46, depth 2790 m. Plane polarized light image.

no-Novogodnyaya BH 210 (core depth 3160–3199 m), it consists of two sandstone beds (17 and 12 m) separated by a bed of silt and clay. Sandstones are strongly carbonatized and rich in cement (few percent to 45–50%). Authigenic carbonates are mostly fine to medium calcite (10–45%) and less abundant fine siderite (2–10%). Authigenic quartz

found as incomplete regeneration rims is very unevenly distributed; its contents correlate with the amount of cement (especially secondary calcite) and grain sizes. Among detrital minerals, 10–15 to 70–80% of quartz clasts are regenerated, but regeneration is rare in rocks with highest contents of cement. Regeneration rims in calcitized sandstones are

corroded. Regenerated detrital quartz makes up 26–37% in weakly carbonatized sandstones from bed U_1^2 and but reaches 56 to 75% in coarser sandstones from U_1^1. The relative percentages of different alteration degrees of pelitized, kaolinized, or less often sericitized feldspars are more or less stable along the section: 5–6% strong, 30–38% moderate, and 56–64% weak alteration. The clay component of cement contains 1–5% of more or less strongly recrystallized authigenic pore kaolinite (very fine to fine and coarse flaky varieties) (Fig. 6*D*, *E*).

The contents of authigenic minerals decrease markedly eastward (Yarainer, Stakhanov, and other areas). Sandstones in the permeable part of the Oxfordian reservoir (Lower Sigovaya Subformation: Upper Tol'ka, Prioozernaya, and West Krasnyi Sel'kup areas) contain lesser amounts of quartz and feldspar. The general pattern of authigenic mineral formation is quite heterogeneous. Only 15–25% of detrital quartz particles have incomplete regeneration rims. Authigenic kaolinite is absent or minor (to 1–2%) in coarser sandstone. Authigenic carbonates occur as interstitial pelitomorphic siderite (few percent to 12%) or calcite (1–10%); the latter occasionally forms strongly calcitized layers with basal cement (up to 40–45%). In the West Krasnyi Sel'kup area (BH 46), 48 to 61% of quartz clasts in medium-grained sandstones from the upper reservoir part (2780–2800 m) are regenerated. The relative percentages of feldspar clasts altered to different degrees (zero or weak, moderate, and strong) are different from the values quoted above: 10, 48 and 42%, respectively, which is typical of sandstones with large stylolitic grain boundaries (Fig. 6*F*) and hydromica-sericite cement. In the case of kaolinite cement (to 3–5%) and less prominent stylolitic sutures, up to 77% of feldspars and only 5–7% of calcites are weakly altered or fresh. Thus, the sediments show signatures of maturation anomalies, possibly produced by cross flow in faulted areas.

CONCLUSIONS

Groundwaters in the Oxfordian regional reservoir of the Nadym–Taz interfluve vary in salinity from almost fresh to weak brines (up to 63.3 g/L) and have mainly sodium chloride to sodium chloride-bicarbonate major-ion chemistry. Primary aluminosilicates of the clastic skeleton lack equilibrium with groundwater and thus are exposed to prolonged continuous dissolution leading to formation of various secondary minerals, while water accommodates elements that fail to bind with the mineral phases (chlorine, sodium, or less often calcium, fluorine, etc.). As water-rock interaction progresses, elements in waters accumulate gradually and unevenly, which induces changes in both authigenic minerals and groundwaters of the respective compositions. The evolution of the water-rock system is controlled mainly by pH and contents of Si, Al, Na, K, Ca, and Mg in the waters. Authigenic minerals form continuously and successively (kaolinite–montmorillonite–illite–micas–chlorite–albite–

microcline). Illite precipitates from waters with lower H_4SiO_4 concentrations while higher-silicic waters produce chlorite phases and secondary albite. The equilibrium between groundwaters and aluminosilicates impinges on the carbonate barrier, and rocks become more or less strongly carbonatized. The assemblages of authigenic minerals include kaolinite in the southern Nadym–Taz interfluve and secondary albite in the north. Authigenic mineral formation generally decays eastward.

Thus, the features of lateral zoning in the salinity and chemistry of groundwaters and in assemblages of authigenic minerals in the Oxfordian reservoir from the Nadym–Taz region allow predicting the distribution of authigenic mineralization which is only locally known from lithological, petrographic, and mineralogical data on core samples. The multidisciplinary studies make another step forward in understanding the geological evolution in the system water-rock-gas-organic matter formulated an age ago by Vladimir Vernadsky.

REFERENCES

Aagaard, P., Helgeson, H.C., 1982. Thermodynamic and kinetic constraints on reaction rates among minerals and aqueous solutions I. Theoretical consideration. Am. J. Sci. 282, 237–285.

Ben Baccar, M., Fritz, B., 1993. Diagenetic albitization of K-feldspar and plagioclase in sandstone reservoirs: thermodynamic and kinetic modeling. J. Sediment. Petrol. 63 (6), 1100–1109.

Bukaty, M.B., 1999. HydrGeo software. Promotional and Engineering Description[in Russian]. VNTITs, Moscow (State Registration of Algorithms and Software at the All-Russian R&D Information Center, No. 50980000051 PC).

Chernikov, O.A., 1969. Alteration of Sand-Silt Sediments and Their Porosity [in Russian]. Nauka, Moscow.

Drever, J.T., 1988. The Geochemistry of Natural Waters (second edition). Prentice Hall, New Jersey.

Fomin, A.N., 2011. The West Siberian Basin: Catagenesis and Petroleum Potential [in Russian]. INGG, Novosibirsk.

Foustoukos, D.I., Savov, I.P., Janecky, D.R., 2008. Chemical and isotopic constraints on water/rock interactions at the Lost City hydrothermal field, 30° N Mid-Atlantic Ridge. Geochim. Cosmochim. Acta 72 (22), 5457–5474.

Frape, S.K., Fritz, P., McNutt, R.H., 1984. Water-rock interaction and chemistry of groundwaters from the Canadian Shield. Geochim. Cosmochim. Acta 48, 1617–1627.

Garrels, R.M., Christ, C.L., 1965. Solutions, Minerals, and Equilibrium. Harper and Row, New York.

Helgeson, H.C., 1969. Thermodynamics of hydrothermal systems at elevated temperatures and pressures. Am. J. Sci. 267 (7), 729–804.

Helgeson, H.C., Knox, A.M., Owens, C.E., Shock, E.L., 1993. Petroleum, oil field waters, and authigenic mineral assemblages: Are they in metastable equilibrium in hydrocarbon reservoirs? Geochim. Cosmochim. Acta 57 (14), 3295–3339.

Hüpers, A., Kasemann, S.A., Kopf, A.J., Meixner, A., Toki, T., Shinjo, R., Wheat, C.G., You, C.-F., 2016. Fluid flow and water–rock interaction across the active Nankai Trough subduction zone forearc revealed by boron isotope geochemistry. Geochim. Cosmochim. Acta 193, 100–118.

Kazansky, Yu.P., Vakulenko, L.G., Solotchina, E.P., Fomin, A.N., 1995. Authigenic mineralogy zoning in Upper Permian (?), Triassic, and Jurassic rocks from the Tyumen superdeep borehole, in: Geology and Petroleum Potential of the Nadym–Pur–Taz Interfluve [in Russian]. Tarko-Sale, Tyumen, pp. 170–179.

Kholodov, V.N., 1982a. New knowledge of catagenesis. Paper I. Infiltration and catagenesis under gravity and salinity effects. Litologiya i Poleznye Iskopaemye, No. 3, 3–22.

Kholodov, V.N., 1982b. New knowledge of catagenesis. Paper II. Catagenesis under compaction and dehydration effects. Litologiya i Poleznye Iskopaemye, No. 5, 15–31.

Kossovskaya, A.G., Shutov, V.D., 1963. Facies of regional epigenesis and metagenesis. Izv. AN SSSR, Ser. Geol., No. 7, 3–18.

Kruglikov, N.M., Nelubin, V.V., Yakovlev, O.N., 1985. Hydrogeology of the West Siberian Basin and Features of Oil and Gas Fields [in Russian]. Nedra, Leningrad.

Lomonosov, M.V., 2012. On the Strata of the Earth [Translated from Russian by Rowland, S.M., Korolev, S.]. Geol. Soc. Am. Spec. Pap. 485.

Lebedev, B.A., 1992. Geochemistry of Postdepositional Processes in Sedimentary Basins [in Russian]. Nedra, Leningrad.

Makhnach, A.A., 1989. Catagenesis and Groundwaters [in Russian]. Nauka i Tekhnika, Minsk.

Makhnach, A.A., 2000. Stadial Analysis of Lithogenesis [in Russian]. Belorus. Gos. Univ., Minsk.

Matusevich, V.M., Rylkov, A.V., Ushatinsky, I.N., 2005. Fluid Systems and Petroleum Potential of the West Siberian Basin [in Russian]. TyumGNGU, Tyumen.

McBride, E.F., 1989. Quartz cement in sandstones: a review. Earth Sci. Rev. 26, 69–112.

McDowell, S.D., Elders, W.A., 1980. Authigenic layer silicate minerals in boreholes Elmore 1, Salton Sea geothermal field, California, USA. Contrib. Mineral. Petrol. 74, 293–310.

Novikov, D.A., 2012. Hydrogeochemical conditions for the formation of authigenic kaolinite in the zone of catagenesis (case study of the Arctic West Siberian basin), in: Geological Evolution of Water-Rock Interaction [in Russian]. NTL, Tomsk, pp. 467–470.

Novikov, D.A., 2016. Hydrogeochemistry of catagenesis in oil and gas reservoirs of the Arctic West Siberian basin. Izv. Vuzov, Neft' i Gaz, No. 6, 19–25.

Novikov, D.A., 2017a. Hydrogeochemistry of the Arctic areas of Siberian petroleum basins. Pet. Explor. Develop. 44 (5), 780–788.

Novikov, D.A., 2017b. Hydrogeological conditions for the presence of oil and gas in the western segment of the Yenisei–Khatanga regional trough. Geodyn. Tectonophys. 8 (4), 881–901.

Novikov, D.A., 2017c. Water–rock interaction in the zone of catagenesis in the Arctic West Siberian basin. Neftegazovoe Delo 15 (1), 40–52.

Novikov, D.A., 2018. Vertical fluid dynamic zoning of the Yamal–Kara basin (northern West Siberia). Izv. Vuzov, Neft' i Gaz, No. 1, 35–42.

Novikov, D.A., Lepokurov, A.V., 2005. Hydrogeological conditions of petroleum potential deposits on the structures in the southern part of Yamalo–Karskoe depression. Geologiya Nefti i Gaza, No. 5, 21–30.

Novikov, D.A., Dultsev, F.F., Chernykh, A.V., 2018a. Abnormally high formation pressures in Jurassic-Cretaceous reservoirs of Arctic regions of Western Siberia, in: IOP Conference Series: Earth and Environmental Science, Vol. 193 (1), p. 012050.

Novikov, D.A., Sadykova, Y.V., Chernykh, A.V., Dultsev, F.F., Sukhorukova, A.F., 2018b. Paleohydrochemistry of Jurassic and Cretaceous deposits in Arctic regions of Western Siberia, in: IOP Conference Series: Earth and Environmental Science. Vol. 193 (1), p. 012051.

Perozio, G.N., 1971. Postdepositional Alteration of Jurassic and Cretaceous Clastic Sediments in the Central and Southeastern West Siberian Basin [in Russian]. Nedra, Moscow.

Predtechenskaya, E.A., 2010. Catagenetic criteria for prediction of low-density zones in Lower–Middle Jurassic deposits in the West Siberian basin. Geologiya i Mineral'no-Syr'evye Resursy Sibiri, No. 3, 35–43.

Predtechenskaya, E.A., Vakulenko, L.G., Zlobina, O.N., 1993. Catagenesis of Lower and Middle Jurassic sandstones in the Urengoi area. Geologiya i Geofizika (Russian Geology and Geophysics) 34 (7), (55–62) 70–79.

Predtechenskaya, E.A., Vakulenko, L.G., Polyakova, I.D., Fomichev, A.S., 2000. Sediment maturity zoning and petroleum potential in the Lower–Middle Jurassic sediments in the Ob'–Taz facies, in: Problems of Lithology, Geochemistry, and Ore Genesis in the Sedimentation Process [in Russian]. GEOS, Moscow, Book 2, pp. 145–149.

Predtechenskaya, E.A., Zlobina, O.N., Burleva, O.V., 2015. Mineralogical and geochemical anomalies as indicators of fluid dynamic processes in Jurassic oil and gas reservoirs of the West Siberian basin. Geologiya, Geofizika and Razrabotka Neftyanykh i Gazovykh Mestorozhdenii, No. 1, 11–24.

Proshlyakov, B.K., 1974. Postdepositional Alteration of Rocks in Oil and Gas Reservoirs [in Russian]. Nedra, Moscow.

Rex, R.V., 1966. Authigenic kaolinite and mica evidence of low temperatures, in: International Series Monographs in Earth Sciences 25, pp. 95–104.

Sakhibgareev, R.S., 1989. Postdepositional Alteration of Rocks during Formation and Degradation of Oil and Gas Reservoirs [in Russian]. Nedra, Leningrad.

Samarina, V.S., 1977. Hydrogeochemistry [in Russian]. Leningrad. Univ., Leningrad.

Scislewski, A., Zuddas, P., 2010. Estimation of reactive mineral surface area during water–rock interaction using fluid chemical data. Geochim. Cosmochim. Acta 74, 6996–7007.

Shvartsev, S.L., 1991. Interaction of water with aluminosilicate rocks: a review. Geologiya i Geofizika (Soviet Geology and Geophysics) 32 (12), 16–49 (13–37).

Shvartsev, S.L., 1995. The problem of self-organization of a water–rock geological system. Geologiya i Geofizika (Russian Geology and Geophysics) 36 (4), 22–29 (17–24).

Shvartsev, S.L., 1998. Hydrogeochemistry of the Zone of Supergene Alteration (second edition)) [in Russian]. Nedra, Moscow.

Shvartsev, S.L., 2008. Interaction in the water-rock system as a new basis for the development of hydrogeology. Russ. J. Pacific Geol. 2 (6), 465–475.

Shvartsev, S.L., Novikov, D.A., 2004. The nature of vertical hydrogeochemical zoning of petroleum deposits (exemplified by the Nadym–Taz interfluve, West Siberia). Geologiya i Geofizika (Russian Geology and Geophysics) 45 (8), 1008–1020 (960–972).

Shvartsev, S.L., Ryzhenko, B.N., Alekseev, V.A., Dutova, E.M., Kondratieva, I.A., Kopylova, Yu.G., Lepokurova, O.E., 2007. Geological Evolution and Self-Organization of the Water–Rock System. Book 2: The Water-Rock System in the Zone of Supergene Alteration [in Russian]. Izd. SO RAN, Novosibirsk.

Silkina, T.N., 2001. Hydrogeochemistry of Oil and Gas Reservoirs in the Nyurol'ka Basin (Tomsk Region). PhD Thesis [in Russian]. Tomsk.

Silkina, T.N., Zhukovskaya, E.A., 2002. Equilibrium with aluminosilicate minerals of groundwaters in Jurassic aquifers of the Nyurol'ka basin, in: Geology and Petroleum Potential of the West Siberian Basin, Proc. 2nd Conf., Part 3 [in Russian]. TNGU, Tyumen, pp. 21–23.

Sirotenko, L.V., 2009. Zones of low density in Jurassic and Permian-Triassic sequences in northern West Siberia (from data of deep and superdeep drilling). Geologiya, Geofizika i Razrabotka Neftyanykh i Gazovykh Mestorozhdenii, No. 11, 66–71.

Sirotenko, L.V., Gorbachev, V.I., 2000. Factors favoring development of petroleum reservoirs in the lower part of the Tyumenskaya superdeep borehole. Geologiya i Geofizika (Russian Geology and Geophysics) 41 (4), 491–502 (478–487).

Stewart, R.N.T., Fallick, A.E., Haszeldine, R.S., 1994. Kaolinite growth during pore-water mixing: isotopic data from Palaeocene sands, North Sea, UK. Clay Minerals 29, 627–636.

Ushatinsky, I.N., Zaripov, O.G., 1978. Petroleum Potential of Mesozoic Deposits in the West Siberian Basin: Mineralogical and Chemical Constraints [in Russian]. Sredneural. Kn. Izd., Sverdlovsk.

Wanner, C., Bucher, K., Pogge von Strandmann, P.A.E., Waber, H.N., Pettke, T., 2017. On the use of Li isotopes as a proxy for water–rock interaction in fractured crystalline rocks: A case study from the Gotthard rail base tunnel. Geochim. Cosmochim. Acta 198, 396–418.

Wilkinson, M., Haszeldine, R.S., Ellam, R.M., Fallick, A., 2004. Hydrocarbon filling history from diagenetic evidence: Brent Group, UK North Sea. Mar. Pet. Geol. 21, 443–455.

Wilson, M.D., Pittman, E.D., 1977. Authigenic clays in sandstones: Recognition and influence on reservoir properties and paleoenvironmental analysis. J. Sediment. Petrol. 47, 3–31.

Yan, P.A., 2001. Structure and composition of the Vasyugan Formation in the Tyumen superdeep borehole (SG-6) section. Geologiya, Geofizika i Razrabotka Neftyanykh i Gazovykh Mestorozhdenii, No. 10, 89–95.

Yan, P.A., Vakulenko, L.G., 1998. Petrography of Callovian–Oxfordian reservoir and cap rocks in the northern latitudinal Ob' basin. Geologiya, Geofizika i Razrabotka Neftyanykh i Gazovykh Mestorozhdenii, No. 7, 9–13.

Yapaskurt, O.V., 2008. Stages in the sedimentation process. Litologiya i Poleznye Iskopaemye, No. 4, 364–376.

Yapaskurt, O.V., Gorbachev, V.I., 1996. Lithogenesis and deep porosity factors in Triassic and Lower–Middle Jurassic sediments from the Tyumen borehole, in: Tyumen Superdeep Borehole (Interval 0–7502 m): Drilling and Investigation Results [in Russian]. KamNIIKIGS, Perm, pp. 194–203.

Yapaskurt, O.V., Shikhanov, S.E., 2007. Models of lithogenesis in synchronously developing Mesozoic basins of different types in northern Siberia. Bull. MOIP. Otd. Geol. 82 (1), 69–81.

Yapaskurt, O.V., Frolov, V.T., Gorbachev, V.I., Dikovsky, A.A., 1992. Postdepositional alteration patterns in Early Mesozoic clastic rocks in the Novyi Urengoi superdeep borehole. Bull. MOIP. Otd. Geol. 67 (1), 73–84.

Yapaskurt, O.V., Kosorukov, V.L., Zolotarev, D.A., 1997. Features of lithogenesis in pre-Cenozoic deltaic-marine facies in basins of different types (northern Siberia). Communication 1. A basin with nearly compensated sedimentation in the Koltogory–Urengoi trough. Litologiya i Poleznye Iskopaemye, No. 1, 36–47.

Zhao, M., Ji, J.F., Chen, Z.Y., Chen, X.M., Cui, X.D., Wang, Y.S., 2011. Evolution of kaolinite subgroup minerals and mixed-layer illite/smectite in the Paleogene Damintum Depression in Liaohe Basin of China and its implication for paleotemperature. Sci. China Earth Sci. 54 (1), 73–83.

Zhukovskaya, E.A., Novikov, D.A., 2002. Equilibrium between groundwater and aluminosilicate minerals in the Oxfordian regional reservoir (case study of the Nyurol'ka basin and the Kharampur swell, in: Thirty Years Working for Tomsk Regional Geology [in Russian]. SNIIGGiMS, Tomsk Filial, Novosibirsk, pp. 279–282.

Zonn, M.S., Dzyublo, A.D., 1990. Jurassic Reservoirs in Northern West Siberia [in Russian]. Nauka, Moscow.

Editorial responsibility: A.E. Kontorovich